Observation of Quasicondensate in Two-Dimensional Atomic Hydrogen

A. I. Safonov,[1,2] S. A. Vasilyev,[2] I. S. Yasnikov,[1,2] I. I. Lukashevich,[2] and S. Jaakkola[1]
[1]*Wihuri Physical Laboratory, Department of Physics, University of Turku, 20014 Turku, Finland*
[2]*Laboratory of Metastable Quantum Systems, ISSSP, Kurchatov Institute, 123182 Moscow, Russia*
(Received 6 February 1998)

We have performed magnetic compression experiments with the two-dimensional gas of hydrogen atoms on liquid ^{4}He at $T = 120-200$ mK. For 2D phase-space densities higher than 3, the probability of three-body dipole recombination is observed to decrease gradually by an order of magnitude in comparison to its low-density value $K_{bbb} = 8.4(3.5) \times 10^{-25}$ cm^4 s^{-1}. This is attributed to local coherence developing in a 2D quasicondensate. We have also determined the value $U/k = 5.1(5) \times 10^{-15}$ K cm^2 for the mean-field energy of the gas. [S0031-9007(98)07787-4]

PACS numbers: 03.75.Fi, 05.30.Jp, 67.65.+z, 68.35.Rh

In addition to the occupation of a single quantum state, a Bose-Einstein condensate (BEC) is characterized by long-range order or, equivalently, global coherence. The concept of quasicondensate (QC) has been introduced [1] for the lesser known situation where a boson system is coherent only locally. Having similar particle interactions, BEC and QC would be hardly distinguishable by virtue of properties related to inelastic [2,3] or elastic [4] collisions. However, the difference is transparent in spatially uniform two-dimensional (2D) system where a BEC cannot exist at finite temperature T but a QC can.

In fact, a QC may appear due to interactions which suppress density fluctuations and therefore allow the 2D system to be described by a single wave function. Although the phase of the function fluctuates spatially and thus thwarts a long-range order [1], the phase coherence persists within a finite length $L \propto \exp(\sigma\lambda^2)$ [2]. Here, $\lambda = \sqrt{2\pi\hbar^2/mkT}$ is the de Broglie wavelength, σ is the 2D gas density, and m is the particle mass. For $T \to 0$ the "local BEC" regions of size L tend to extend throughout the sample and the QC turns into a "true" condensate.

The appearance of a QC is to be expected when the interaction energy becomes comparable with the kinetic energy, $\sigma U \sim kT$. Here, $U = 4\pi\hbar^2\xi/m$ is the mean-field parameter for elastic interactions and ξ is a dimensionless interaction strength. It is known that at $T = 0$ the ratio of densities of above-condensate and condensate particles is $\sigma'/\sigma_0 \approx \xi$ [5]. Therefore a QC may manifest itself preferably in weakly interacting (low-ξ) systems.

This Letter reports on the first experimental evidence for a quasicondensate in 2D atomic hydrogen gas, where we have observed a significant reduction in three-body recombination probability [2,6]. Hydrogen atoms on liquid ^{4}He surface occupy a single bound state with low adsorption energy, $E_a/k \simeq 1.0$ K [7]. The H adatoms are localized quite far, 8 Å, from the liquid and their out-of-plane delocalization length, $l = \hbar/\sqrt{2E_a m} \simeq 5$ Å, is large compared with, e.g., the 3D scattering length $a_0 = 0.72$ Å. Thus adsorbed hydrogen may be also regarded as quasi-2D in the sense that it obeys 2D statistics while particle interactions are three dimensional [2]. It may be shown [2] that $\xi \approx a_0/l$ and consequently a QC in hydrogen on ^{4}He may be observed at $\sigma\lambda^2 \gtrsim l/2a_0 \simeq 3.5$.

It is not easy to achieve a high degree of quantum degeneracy, i.e., high σ at low T, in atomic hydrogen that is metastable with respect to recombination into molecules [7]. The sample quickly decays and the huge energy released, $D = 4.5$ eV/H$_2$, causes an essential rise in T. Recombination may be suppressed by polarizing electron spins in a strong magnetic field B at low temperature. However, the ground hyperfine state a is mixed containing a slight fraction of the opposite spin orientation ($\uparrow$) [7], and such atoms are prone to recombine with each other or with atoms in the "pure" state b. The latter cannot recombine via bb collisions. This preferential depletion of the a population leads to the formation of a more stable, predominantly b-state sample.

A QC in 2D $H\downarrow$ may be detected by comparing the rates of two different processes. One of them is a three-body (bbb) dipole recombination [6], the dominating and unavoidable channel of the sample decay at high densities. In a fully condensed sample its probability would be suppressed by a factor of 3! [8]. The other is a two-body (ab) exchange recombination which involves *distinct* atoms and is therefore not affected by the formation of a QC. We induce exchange recombination by rf pulses flipping nuclear spins and thus converting a small fraction of b atoms to the a state [9]. The resulting recombination is seen in the atom loss rate as peaks on the background of the dipole contribution. Each peak decays while the induced a atoms recombine with b atoms. The relaxation time of a peak is the lifetime τ of the flipped atoms and serves as the measure of the ab recombination rate. For an ideal Boltzmann gas a log-log plot of the bbb rate vs the ab rate would be a straight line with the slope 3/2.

To overcome problems with excessive heating and fast loss of the H sample due to recombination, we used the idea of local compression [10]. An annular ring of dense 2D $H\downarrow$ is collected on the $\Delta R = 20(1)$ μm wide, 0.3 cm diameter

upper rim of a 1 cm long FeCo (Permendur) field intensifier tube (Fig. 1). This provides a heat transfer path of more than an order of magnitude shorter than in our previous experiment [9]. In the ^{4}He level position indicated in Fig. 1 the rim face (area $A_r = 2 \times 10^{-3}$ cm^2) is covered with a saturated ^{4}He film and the $H\downarrow$ atoms experience almost a constant field enhancement $\Delta B \simeq 2$ T over the radial distance ΔR. In this way a nearly rectangular 1.5 K deep and 20 μm wide potential well is formed. When more helium is pushed into the cell, the gap between the Cu rings is suddenly filled by liquid, and compression is stopped.

The loss rate of $H\downarrow$ atoms (Fig. 2) is detected via its energy yield using a carbon bolometer [9,11,12] placed in the buffer volume ($V = 4.5$ cm^3). The bolometer response is calibrated against a temperature controller and a 128 GHz (ambient field $B_0 = 4.57$ T) ESR spectrometer [9,12]. The use of the bolometer is based on the observations [11,13,14] that only of order 1% of D is released locally at the recombination site. In the present experiment the mean free path is so long that excited hydrogen molecules undergo hundreds of wall collisions before relaxing to the ground state [11]. Thus the molecules distribute their energy evenly over the whole cell surface including the bolometer. The free surface of the liquid ^{4}He bath in the cell is small and the rest of the inner cell surface (area $A_0 = 22$ cm^2) is wetted by a ^{4}He film. The large recombination heat flux, up to 1 μW/cm^2, through a Kapitza resistance causes a temperature difference $T_f - T_0 \leq 10$ mK between the film and the cell body. On the other hand, the temperature of the bulk liquid does not exceed T_0 by more than 1 mK.

To analyze the experimental data on the recombination rates, one has to know accurately the adsorption energy E_a, magnetic field enhancement ΔB at the intensifier rim, the intrinsic rate constant of exchange recombination K_{ab}, and the effective rate constant G_1 of first-order nuclear relaxation.

Without magnetic compression and rf pulses, the decay of the buffer volume density n is controlled by a $b \rightarrow a$ relaxation due to magnetic impurities in the cell walls followed by much faster ab recombination.

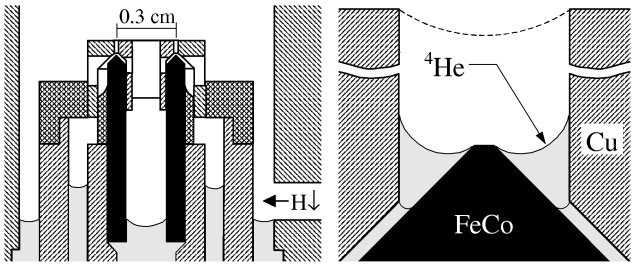

FIG. 1. Sample cell with tubular field intensifier (left) and design of the compression region (right). ESR and NMR cavities, thermal sensors, and the liquid level control system are not shown.

One then has $dn_a/dt = G_1 n_b - K_{ab}^{\rm eff} n_a n_b$ for a atoms whose steady-state density is small, $n_a^{\rm st} = G_1/K_{ab}^{\rm eff} \ll n_b$. Now we observe $G_1 = 3.6 \times 10^{-3}$–7×10^{-4} s^{-1} from purely exponential decays $dn_b/dt = -2G_1 n_b$ at $T_0 = 120$–200 mK.

The inverse lifetime of the induced a atoms ($n_a - n_a^{\rm st} \ll n_a^{\rm st}$) measured with a closed compressor is linear in density, $\tau_0^{-1} = K_{ab}^{\rm eff} n_b + 4\gamma G_1$. The slope of this line is the effective rate constant $K_{ab}^{\rm eff}$ while the intercept gives $\gamma \equiv K_{aa}^{\rm eff}/K_{ab}^{\rm eff} = 4.4(2.6)$ for the ratio of probabilities of aa and ab recombinations. Assuming $K_{ab} \propto \sqrt{T}/B^2$, the temperature dependence

$$K_{ab}^{\rm eff} = K_{ab}(A_0/V)\lambda^2 \exp(2E_a/kT_0), \qquad (1)$$

yields $E_a/k = 1.01(3)$ K and $K_{ab} = 1.8(8) \times 10^{-9}\sqrt{T}$ cm^2 K$^{-1/2}$ s^{-1} (in $B_0 = 4.57$ T), in agreement with data given elsewhere [7,9,12].

The average field enhancement is determined in the same way as E_a but with an open compressor [9]. To do so, a homogeneous temperature must be ensured by keeping n_b low enough. Then $\tau^{-1} \simeq K_{ab}^{\rm eff} n_b (1 + A_r^{\rm eff}/A_0)$, where the effective area of the magnetic ring is $A_r^{\rm eff} = A_r(1 + \Delta B/B_0)^{-2} \exp(2\mu_B \Delta B/kT_0)$. A numerical fit gives $\Delta B = 2.00(2)$ T in agreement with $\Delta B = 1.98(6)$ T measured with a 3×3 μm Hall probe at 3 μm above the middle of the intensifier pole face. We actually estimate that in the course of experiments the face will be coated with a couple-of-microns-thick H_2 layer.

There are three hydrogen subsystems in the cell with different temperatures and chemical potentials: dilute 3D gas in the buffer (T_f, μ_f), dense but still classical 3D gas in the well (T_3, μ_3), and possibly degenerate 2D gas adsorbed on the helium surface (T_2, μ_2). When the intensifier is open, most recombination events take place at the magnetic ring and, at high densities (high loss rates), heat the adsorbed $H\downarrow$ considerably above T_f. The molecules leave a part of their excitation energy in the 3D gas in the well and heat it above T_2.

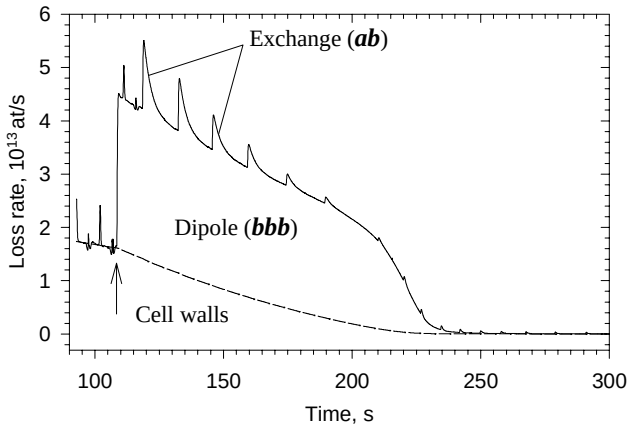

FIG. 2. Evolution of the loss rate of atoms detected by a bolometer. Various contributions are indicated. The arrow points to the opening of the intensifier.

The chemical potential of the buffer gas is $\mu_{f\nu} = kT_f \ln(n_\nu \lambda_f^3)$ while for the 3D gas in the well we have $\mu_{3\nu} = kT_3 \ln(n_\nu \lambda_3^3) - \mu_B \Delta B$. Here ν denotes the hyperfine state a or b. The loss rate is much smaller than the rate of particle exchange between the well and the buffer and may therefore be neglected when considering a stationary density distribution. Thus equating atomic fluxes in opposite directions gives $T_f^2 \exp(\mu_f/kT_f) = T_3^2 \exp(\mu_3/kT_3)$ and $T_3^3 \exp(\mu_3/kT_3) = T_2^3 \exp(\mu_2/kT_2)$. The latter relation implies that the sticking probability of an H atom on ^{4}He is $0.3T/\mathrm{K}$ [7]. Finally, we obtain $\mu_f/kT_f = \mu_2/kT_2 + \ln(T_2^3/T_3T_f^2)$, where the logarithmic term is $\ll 1$ and may be omitted because $T_3 \geq T_2 \geq T_f$ and the relative temperature difference is small.

Noting that $\sigma_a \lambda_2^2 \ll 1$ and that, in the absence of a (quasi)condensate, the interaction of distinct particles (a and b) is twice as weak as that of identical particles (b and b), given the same interaction potential, we may write for the chemical potential of the 2D gas (compare with [15]).

$$\mu_{2a} = kT_2 \ln(\sigma_a \lambda_2^2) + U\sigma_b - E\,, \tag{2a}$$

$$\mu_{2b} = kT_2 \ln[1 - \exp(-\sigma_b \lambda_2^2)] + (2 - \theta)U\sigma_b - E\,, \tag{2b}$$

where $E \equiv \mu_B \Delta B + E_a$. By analogy with the three-body correlator [8], θ is the square of the quasicondensate fraction. It grows from zero to its $T = 0$ value [2] $(1 - \xi)^2 \approx 0.7$ starting at $\sigma\lambda_r^2 = 3$ (see below). The first terms of Eqs. (2a) and (2b) are accurate only when there is no QC. When there is, these kinetic terms are small compared to the interaction term and the corresponding correction to $\mu_{2\nu}$ is insignificant.

In a general case (open compressor, arbitrary density, and therefore nonuniform temperature in the cell), the lifetime of NMR-induced a atoms satisfies the equation

$$\tau^{-1} = \tau_f^{-1} + \frac{A_r \sigma_a}{V n_a}(K_{ab}\sigma_b + K_{abb}\sigma_b^2)\,, \tag{3}$$

where $\tau_f = \tau_0(T_f \neq T_0)$ stands for the contribution of the buffer volume walls. The rate constant K_{abb} refers to the recombination of a atoms with two b atoms which might be important at high σ_b.

By separating the contribution of the compression ring, $\tau_r^{-1} = \tau^{-1} - \tau_f^{-1}$, we define a reduced exchange rate $L_{\mathrm{ex}} = Vn_b/\tau_r$. Using equations for μ_f and μ_3 and Eqs. (2), we may express it in the form

$$L_{\mathrm{ex}} = \frac{A_r}{\lambda_2^2}(K_{ab}\sigma_b + K_{abb}\sigma_b^2)[1 - \exp(-\sigma_b\lambda_2^2)]F\,, \tag{4}$$

where $F \equiv \exp[(1 - \theta)U\sigma_b/kT_2]$. At low densities, $L_{\mathrm{ex}} = A_r K_{ab}\sigma_b^2$ which immediately gives the surface density. We define the dipole rate as $L_3 = -Vdn_b/dt - 2G_1 n_b$ and undoubtedly

$$L_3 = A_r K_{bbb}\sigma_b^3\,. \tag{5}$$

We emphasize that L_{ex} and L_3 are direct experimental quantities characterizing the processes at the compression surface, which should react differently to the appearance of a QC. It is also notable that Eq. (4) does not contain the strong exponent $\exp(E/kT_2)$ which would lead to an order of magnitude uncertainty even for a small variation in T_2.

In order to find K_{abb}, K_{bbb}, and U, we fit the experimental data for L_{ex} and L_3 (Fig. 3) to Eqs. (4) and (5) as parametric functions of σ_b with $\theta = 0$ (no QC). Only data below the kink (138 points out of 217) were used. The fit (solid line) gives $K_{bbb} = 7.2(4) \times 10^{-25}\ \mathrm{cm^4\,s^{-1}}$, $U/k = 5.1(5) \times 10^{-15}\ \mathrm{K\,cm^2}$ and $K_{abb} = 0(1) \times 10^{-24}\ \mathrm{cm^4\,s^{-1}}$ (compare with [6]). Extrapolation of the fit to higher rates beyond the kink results in a marked discrepancy with the experiment which is not eliminated by varying K_{abb}, K_{bbb}, and U within their error bars. When we fit *all* of the data, the quality of the fit becomes poor (dashed line, Fig. 3). In fact, the dependence of L_{ex} on K_{abb} and U is too smooth to explain the abrupt change of the slope of the experimental data seen in Fig. 3.

We extract the surface density σ_b from Eq. (4) and then determine K_{bbb} from Eq. (5). For that purpose we combine Eqs. (2a) and (3) with the expression for μ_f and obtain

$$kT_2 = (U\sigma_b - E)/\ln(A_r\lambda_f K_{ab}\sigma_b/V)\,, \tag{6}$$

where the three-body recombination involving a atoms and the temperature dependence of the logarithm are neglected. Equations (6) and (4) are solved numerically with respect to σ_b and T_2. As expected, T_2 grows almost linearly with the loss rate of atoms (Fig. 4). This supports our analysis and confirms that the value of ΔB is correct.

The results for the three-body dipole recombination rate constant K_{bbb} are presented in Fig. 3 as functions of the 2D degeneracy parameter up to the largest value $\sigma\lambda_2^2 = 8.9(6)$

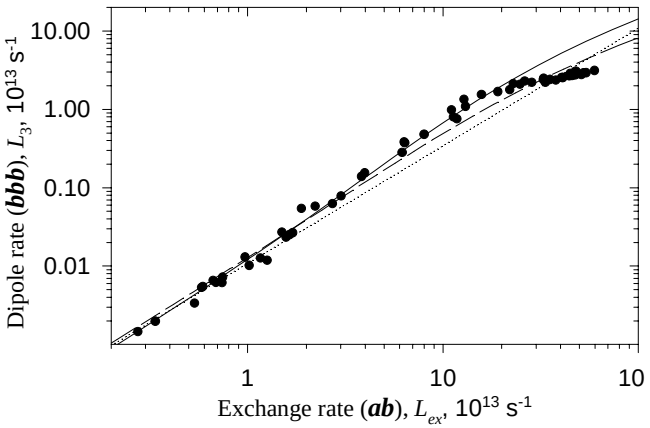

FIG. 3. Dipole (L_3) vs exchange (L_{ex}) rates for $T_0 = 150$ and 162 mK. The solid line is the fit of the data below the kink to Eqs. (4) and (5) with $\theta \equiv 0$. The dashed line is the same fit of all data. The dotted line represents an ideal Boltzmann gas.

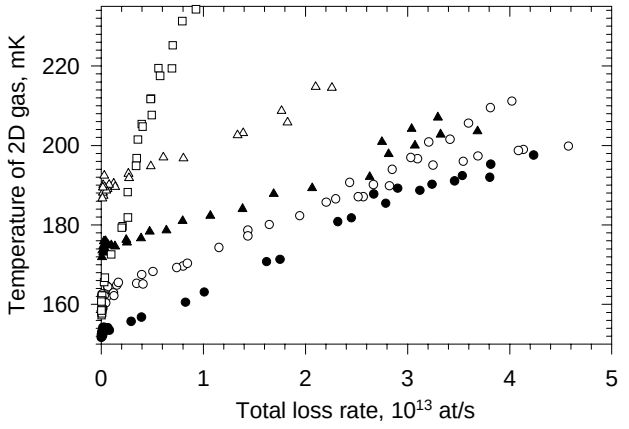

FIG. 4. Temperature of the 2D gas for $T_0 = 150$ (●), 162 (○), 174 (▲), and 190 (△) mK. The data for an earlier intensifier [9] (□) are reduced to the present compression area.

obtained here at $T_2 = 202(2)$ mK and $\sigma_b = 5.9(4) \times 10^{13}$ cm^{-2}. At low densities, K_{bbb} remains constant, $K_{bbb} = 8.4(3.5) \times 10^{-25}$ cm^4 s^{-1}, which agrees with the above fitting result and data given elsewhere [16]. However, starting at $\sigma_b \lambda_2^2 \approx 3$, K_{bbb} decreases steadily and at the highest degeneracy it is suppressed by a factor of 11(2). We believe that, like the distinct bending of L_{ex} in Fig. 3, this is caused by a QC developing in the degenerate 2D $H\downarrow$ gas. We emphasize that the degeneracy at which the decline in K_{bbb} begins agrees with the above estimate $\sigma\lambda^2 \sim l/2a_0$ for the appearance of a QC.

The suppression of K_{bbb} is about twice as large as the expected 3! and does not show saturation. This may be qualitatively explained by the spreading of the wave function of adsorbed H atoms in the out-of-plane direction when the surface coverage is a noticeable fraction of its limiting value $\sigma_{\mathrm{sat}} \simeq (4\pi a_0 l)^{-1} \simeq 2 \times 10^{14}$ cm^{-2} [17]. As repulsive interactions reduce E_a by roughly $U\sigma_b$, the delocalization length increases and the collision probability decreases accordingly. However, delocalization alone cannot explain the observed reduction in K_{bbb}, because it grows smoothly with density. Besides, the highest density obtained here is only about 30% of σ_{sat}, and the corresponding suppression of K_{bbb} [17] would be much smaller than observed.

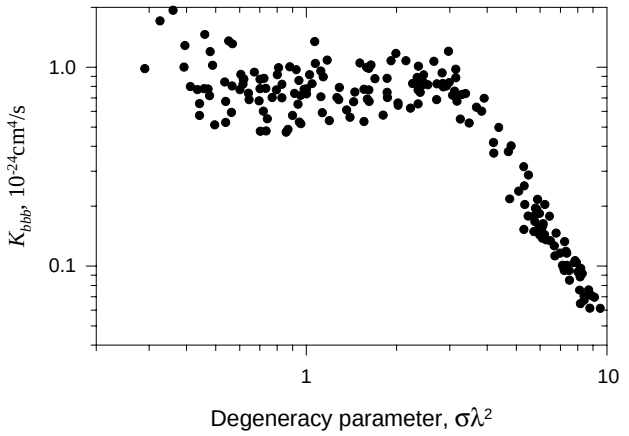

FIG. 5. The rate constant K_{bbb} of three-body dipole recombination as a function of a 2D degeneracy parameter.

The value of the mean-field parameter U is important for our data analysis. The above-mentioned first experimental result for U in 2D hydrogen agrees with theory [2]. Even for a 50% larger U, i.e., far outside the error bar, the decline of K_{bbb} for $\sigma_b \lambda_2^2 > 3$ persists, although it becomes twice as small. At the same time for $\sigma_b \lambda_2^2 < 3$, K_{bbb} increases with growing degeneracy which is physically unreasonable.

The relation of the observed phenomenon to 2D superfluidity is not yet clear. Further theoretical and experimental studies are needed to clarify the physical meaning of the quasicondensate. Therefore experiments with direct optical observation of 2D atomic hydrogen [18] seem promising.

We thank Yu. Kagan, S. Shevchenko, and B. Svistunov, and especially M. Reynolds for valuable discussions, as well as P. Arvela, S. Boldarev, A. Frolov, and E. Tjukanoff for their contributions. Grants from INTAS, RFBR, Wihuri Foundation, and Russian Ministry of Science and Technology are also gratefully acknowledged.

[1] V. N. Popov, *Functional Integrals in Quantum Field Theory and Statistical Physics* (Reidel, Dordrecht, 1983).
[2] Yu. Kagan, B. V. Svistunov, and G. V. Shlyapnikov, Sov. Phys. JETP **66**, 314 (1988).
[3] E. A. Burt *et al.*, Phys. Rev. Lett. **79**, 337 (1997).
[4] W. Ketterle and H.-J. Miesner, Phys. Rev. A **56**, 3291 (1997).
[5] M. Schick, Phys. Rev. A **3**, 1067 (1971).
[6] Yu. Kagan, I. A. Vartanyants, and G. V. Shlyapnikov, Sov. Phys. JETP **54**, 590 (1981).
[7] For a review, see J. T. M. Walraven, in *Fundamental Systems in Quantum Optics*, edited by J. Dalibard, J. M. Raimond, and J. Zinn-Justin (Elsevier, Amsterdam, 1992), p. 485.
[8] Yu. Kagan, B. V. Svistunov, and G. V. Shlyapnikov, JETP Lett. **42**, 209 (1985).
[9] A. I. Safonov *et al.*, JETP Lett. **61**, 1032 (1995).
[10] Yu. Kagan and G. V. Shlyapnikov, Phys. Lett. A **130**, 483 (1988).
[11] S. A. Vasilyev *et al.*, Europhys. Lett. **24**, 223 (1993).
[12] M. Mertig *et al.*, J. Low Temp. Phys. **100**, 45 (1995).
[13] A. Matsubara *et al.*, Physica (Amsterdam) **194B-196B**, 899 (1994).
[14] E. S. Meyer *et al.*, Phys. Rev. B **50**, 9339 (1994).
[15] B. V. Svistunov *et al.*, Phys. Rev. B **43**, 13 412 (1991).
[16] D. A. Bell *et al.*, Phys. Rev. B **34**, 7670 (1986).
[17] Yu. Kagan *et al.*, Phys. Lett. A **135**, 219 (1989).
[18] A. P. Mosk *et al.*, J. Low Temp. Phys. (to be published).